Ginsenoside Rg1-Notoginsenoside R1-Protocatechuic aldehyde attenuates low shear stress-induced vascular endothelial cell dysfunction

Lei Zhang
First Clinical Medical College, Shandong University of Traditional Chinese Medicine.
Yuan Li
Experimental Center, Shandong University of Traditional Chinese Medicine.
Xin Ma
First Clinical Medical College, Shandong University of Traditional Chinese Medicine.
Xiaojie Wang
First Clinical Medical College, Shandong University of Traditional Chinese Medicine
Lingxiao Zhang
First Clinical Medical College, Shandong University of Traditional Chinese Medicine.
Yunlun Li
Experimental Center, Shandong University of Traditional Chinese Medicine. Affiliated Hospital of Shandong University of Traditional Chinese Medicine.
Wenqing Yang (wenqing-yang@hotmail.com)
Experimental Center, Shandong University of Traditional Chinese Medicine https://orcid.org/0000-0003-4622-7393

Research

Keywords: atherosclerosis, endothelial dysfunction, Piezo1, Ginsenoside Rg1-Notoginsenoside R1-Protocatechuic aldehyde

Posted Date: May 4th, 2020

DOI: https://doi.org/10.21203/rs.3.rs-25782/v1

Abstract

Background

The Fufang Danshen formula is widely used in traditional Chinese medicine for the clinical treatment of coronary heart disease. However, there is no literature reporting the anti-atherosclerotic effect and mechanism of its combination of active ingredients, namely Ginsenoside Rg1-Notoginsenoside R1-Protocatechuic aldehyde (PPR). The aim of this study was to investigate the anti-atherosclerotic effects in ApoE$^{-/-}$ mice and potential mechanism of PPR in low shear stress-injured vascular endothelial cell.

Methods

In vivo assay, ApoE$^{-/-}$mice were randomly divided into three groups: model group, Rosuvastatin group, and PPR group, with C57BL/6J mice as control group. A variety of staining methods were utilized for the observation of aortic plaque. The changes of the blood lipid indexes were observed by an automatic biochemistry analyzer. ET-1, eNOS, TAX_2, and PGI_2 were analyzed by enzymelinked immunosorbent assay. In vitro, we used fluid shear system to induce cell injury and silenced Piezo1 expression in HUVECs by siRNA. We observed the morphological, proliferation, migration and tube formation activity changes of cells after PPR intervention. Quantitative Real-Time PCR and western blot analysis was applied to observe m RNA and protein expression.

Results

Results showed that PPR treatment reduced atherosclerotic area and lipid level and improved endothelial function in ApoE$^{-/-}$ mice. PPR significantly repaired cell morphology, reduced cell excessive proliferation and ameliorated migration and tube formation activity. In addition, we found that PPR could affect FAK-PI3K/Akt signaling pathways. Importantly, Piezo1 siRNA abolished the protection effects of PPR.

Conclusions

In summary, our results suggested that PPR ameliorated atherosclerotic plaque formation and endothelial cell injury by intervening the FAK-PI3K/Akt signaling pathways. Piezo1 is a possible target of PPR in the treatment of atherosclerosis. These results indicate that PPR may be apotential drug for atherosclerosis.

Background

In recent years, with the change of people's living standard and diet structure, coronary heart disease and ischemic stroke has been increased, which lead to increase risk of major adverse cardiovascular events (MACEs)[1]. Maces are closely related to atherosclerotic plaque progression and rupture. Atherosclerosis

is a chronic inflammatory disease characterized by dyslipidemia, foam cell formation and lipid plaque accumulation in the artery wall.[2, 3]. Vascular endothelium cell (VECs) is an important locus of critical regulatory nodes in homeostatic network of cardiovascular system [4, 5]. In disease, endothelial cell dysfunction within the walls is an important contributor to the local and systemic manifestations of atherosclerotic cardiovascular disease [6, 7]. Fluid mechanical forces generated by arterial blood flow could act directly on endothelial cells to alter their morphological and functional properties. Many researches suggested that distinct hemodynamic forces might constitute a local risk factor for endothelial cell dysfunction in atherogenesis [8]. Thus, shear stress is a potential target for finding an anti-atherosclerotic drug.

Phosphatidylinositol 3-kinase (PI3K) is an important component of the signal transduction in growth factor receptor superfamily. PI3K can be activated by a variety of cytokines and physical and chemical factors. PI3K will phosphorylate and activate downstream cytokines such as Akt, rotein kinase C, and phosphoinositide-dependent kinase 1, among which Akt, which will activate endothelial nitric oxide synthase (eNOS) to produce nitric oxide (NO), is the most important [9]. PI3K/Akt signaling pathway plays a key role in various cellular processes, including cell survival, growth, and proliferation [10]. In addition, PI3K/Akt signaling pathway complex be used as a biomarker with predictive and prognostic values [11, 12]. The Piezo1 protein ion channel is a novel mechanical activated ion channel, which has the ability to sense mechanical signals and regulate cell volume homeostasis [13]. Piezo1 is widespread in VECs and plays a key role in the regulation of cardiovascular development and physiological function. Piezo 1 can be activated by shear forces caused by blood flow [14]. Previous studies have shown that laminar shear can activate piezo1 to regulate the release of NO from endothelium, thus affecting the local vascular tension and playing an anti atherosclerotic role [15]. However, if the VECs are affected by eddy current, the activated piezo1 will promote the development of atherosclerosis through NF-κB pathway [16, 17].

Fufang Danshen formula is the clinically important anti-atherosclerosis drugs. Ginsenoside Rg1 (Rg1), Notoginsenoside R1 (R1), and Protocatechuic aldehyde (PCAD) were its main active components of anti-atherosclerosis. We have previously found that monomer combinations, namely Rg1-R1-PCAD (PPR), have the effect of protecting endothelial cells and the preliminary mechanism may attribute to decrease inflammatory reaction and reducing cell permeability. However, the possible mechanisms have not yet been elucidated. Based on the aforementioned evidence, we investigated that PPR intervened ApoE$^{-/-}$ mice to verify the anti-atherogenic effect. To deeply elucidate the beneficial mechanisms of PPR, we explored the endothelial cell protective effects against low shear stress-induced injury. Our results suggested that PPR ameliorated atherosclerotic plaque formation and endothelial cell injury by intervening the FAK-PI3K/Akt signaling pathways. Piezo1 is a possible target of PPR in the treatment of atherosclerosis. These results indicate that PPR may be apotential drug for atherosclerosis .

Materials And Methods

The Preparation of Rg1, R1, and PCAD

Rg1 (Dalian Meilun Biotechnology Co., LTD. China), R1 (Shanghai standard biotechnology, China), and PCAD (Dalian Meilun Biotechnology Co., LTD. China) were dissolved in dimethyl sulfoxide and then diluted with DMEM·F12. The solution was stored at 4 °C.

Animal experiments

Aged 8 weeks male ApoE$^{-/-}$mice (23.12 ± 1.18 g) and aged 8 weeks male C57BL/6 mice (22 ± 2.2 g) were purchased from Beijing weitonglihua experimental animal technology co., Ltd. (Beijing, China). The animal certificate number was SCXK (Jing) 2014-0004. The animal experiments were performed in accordance with the Guide for the Care and Use of Laboratory Animals (published by the US National Institutes of Health) and were approved by the Institutional Animal Care and Research Advisory Committee of the Shandong University of Traditional Chinese Medicine. All experimental procedures were performed in strict accordance with the international regulation of animal welfare. All mice were maintained under SPF laboratory conditions with free water and food ad libitum, at a temperature of 22 ± 2 °C on a 12 h light/dark cycle during the experimental period. After 1 week of adaptation, all the mice were fed with high-fat diet including 0.15% cholesterol and 21% pork fat. After 12 weeks of continuous feeding, ApoE$^{-/-}$ mice were randomly divided into three groups, with 10 mice in each group: model group (vehicle; Nacl, i.p.); rosuvastatin group (positive-control group, 10 mg·kg^{-1}, i.g.) and PPR group [(10mgRg_1 + 10mgR_1 + 14 mg PCAD)·kg^{-1}, i.p.]. 10 C57BL/6J mice were used as control group (vehicle; Nacl, i.p.). All animals were administered once daily continuously for 8 weeks.

Specimen Collection And Processing

After 8 weeks of intervention, mice were weighed, fasted overnight, anesthetized using isoflurane, and euthanized. Fresh blood samples were collected from the left ventricle. Serum was separated by centrifugation at 3500 r·min^{-1} for 15 min at 4 °C. After the blood collection, the thoracic and abdominal cavity was quickly opened to expose the heart and perfusion the cardiovascular system. The aortas from the aortic arch to left and right common iliac artery were separated and excess tissues outside the vessels were carefully removed. The aortic root and part of the myocardial tissue were taken and fixed in 4% paraformaldehyde. Aorta samples were removed and stored at -80 °C or soaked in 4% paraformaldehyde.

Pathological Morphology Analysis

The en face aortic was stained with Oil-red O and to assess overall burden and distribution of atherosclerosis. Briefly, the whole aorta was opened longitudinally, pinned flat, and fixed in 4% paraformaldehyde solution overnight. Then, the aorta was washed 3 min with PBS and was stained with 0.5% Oil-red O working solution for 60 min at 37℃ biochemical incubator. Subsequently, the aorta was immersed into 70% ethanol for destaining and then was rinsed with PBS. The images were captured by a stereomicroscope. The extent of aortic atherosclerosis was evaluated as the ratio of lesion area to aorta

area. Then, the aortic sinus was fixed with 4% paraformaldehyde solution for 24 h for later paraffinization. The aortic sinus were sliced into 5 μm serial paraffin sections. H&E, Masson and Movat staining (room temperature) were performed on the aortic sinus section samples to determine aorta lipid plaque areas, collagen fiber content, and elastin plaque area respectively. At least five sections for each animal in one group were evaluated, and the lesion was calculated from eight different mice. Images were observed and collected under a microscope (ZEISS, Germany). All images were quantified using the Image-pro plus 6.0 (Media Cybernetics, USA)

Determination Of Serum Lipid Concentration

Serum concentrations of total cholesterol (TC), triglyceride (TG), high-density lipoprotein cholesterol (HDL-C) and low-density lipoprotein cholesterol (LDL-C) were detected by a ZY-310 Automatic Biochemistry Analyzer (Shanghai Kehua Bio-engineering, Shanghai, China) according to the manufacturer's instructions. The atherosclerosis index (AI) was derived as AI = non-HDL-C/HDL-C.

Determination Of Serum Biochemical Parameters

Serum concentrations of eNOS, endothelin-1 (ET-1), Prostaglandine2 (PGI_2) and ThromboxaneA2 (TXA_2) were determined according to manufacture protocol by enzyme-linked immunosorbent assay (ELISA) reagent kits (Elabscience Biotechnology, Wuhan, China).

Cell Culture

The human umbilical vein endothelial cell line (8000) was purchased from ScienCell Research Laboratories (Carlsbad, CA). HUVECs were cultured in endothelial cell medium (ECM) containing 5% FBS, 1% ECGS and 1% P/S Solution (ScienCell, California, USA). Cells were maintained at 37 °C and 5% CO_2 in a humidified incubator. HUVECs from passages 2 to 5 were used for the experiments.

Shear Stress Experiments

Shear stress was applied to confluent HUVECs using an Ibidi pump system (Ibidi, Munich, Germany). Special channel slides of Ibidi (μ-Slide I $^{0.4}$ Luer) were used to expose cells to laminar shear stress. 250,000 primary HUVECs were seeded onto a μ-Slide I $^{0.4}$ Luer and incubated for 24 h at 37 °C and 5% CO_2 in the incubator to form a monolayer. And then flow chambers were then connected to a peristaltic pump. The Ibidi pump system was set up per the company’s instructions and proprietary software was used to control the level of shear applied to cells by controlling total media flow rate through the channels of known dimensions. The experiment was conducted under the following conditions: 6-mbar pressure, 2.5 $mL \cdot min^{-1}$ flow rate and a shear stress of 4 dyn/cm^2.

siRNA Transfection

The cells were transfected with siRNA using a transfection reagent according to the manufacturer's protocol. Briefly, siRNAs and the transfection reagent were added to the medium, followed by incubation for 6 hours at 37 °C. The medium was carefully removed, and ECM with 5% FBS was added. The cells were then incubated at 37 °C in a humidified atmosphere of 5% CO_2 and 95% air for 24 h-48 h for subsequent experiments. To evaluate the efficiency of transfection, cells transfected with a control siRNA (FITC, fluorescein conjugate) was visualized by a fluorescent microscope (ZEISS, Germany).

Immunofluorescence

The F-actin in HUCVECs was examined by immunofluorescence to observe cell morphology. Cells grown on flow chambers were fixed with 4% paraformaldehyde in PBS for 10 min at room temperature (RT) and washed three times with PBS. Cells were then permeabilized with 0.1% Triton X-100 in PBS for 5 min and blocked for 30 min with 1% bovine serum albumin (BSA). F-actin antibody (KeyGEN BioTECH, Jiangsu, China, 1:40 dilution) was added and incubated in the dark for 20 min at RT. After being washed with PBS, the nuclei were stained with DAPI (Abcam, USA) in the dark for 5 min at RT. Cells were observed and collected under a microscope (ZEISS, Germany).

Proliferation Ability Assay

HUVECs Proliferation ability was tested using CCK-8 according to the manufacturer's instructions. HUVECs were diluted to 8×10^4/mL and 100μL cell suspension was added to 96-well plates. After 24 h, the culture medium was sucked out, and then cells incubated with CCK-8 reagent for 1 h at 37 °C. The absorbance was measured at 450 nm by a microplate reader (BioTek, USA).

Migration Assay

HUVECs migration rate was determined using a transwell chamber (Coning, USA). HUVECs were diluted to 1×10^5/mL with serum-free medium and 200 μL cell suspension was added to upper compartment. 0.5 mL 5% FBS contained ECM medium was added to the lower chamber. The upper chamber was put in the lower chamber, and cultured for 6 h at 37℃. Using a dry cotton swab to wipe the remaining cells on the upper chamber, the cells on the underside of the membrane of the upper chamber were fixed with 4% paraformaldehyde for 30 min. And then the cells were stained with hematoxylin staining solution and eosin staining solution for 30 and 10 min respectively. Images were observed and collected under a microscope (ZEISS, Germany) and quantified using the Image-pro plus 6.0 (Media Cybernetics, USA). The number of HUVECs migrated from the upper compartment to the lower compartment was counted.

Tube Formation Assay

HUVECs tube formation experiment was performed using a In Vitro Angiogenesis Tube Formation Assay Kit (Trevigen, USA). 50 μL of BME at 4 °C was added into each well of a 96-well plate and polymerized for 1 h at 37 °C. HUVECs were diluted to 1×10^4/mL with serum-free medium and 100 μL cell suspension was added to the top of the gel and incubated at 37 °C in a humidified chamber with 5% CO_2. After 4 h, the culture medium was sucked out, and washed with PBS. 100 μL of Calcein AM (2 μM) was added into each well and the formation of capillary-like tubes was observed after 30 min. Images were observed and collected under a microscope (ZEISS, Germany) and the numbers of junctions and segments and the length of the network were calculated using the Image-pro plus 6.0 (Media Cybernetics, USA).

Western Blot Analysis

HUVECs were lysed with cell lysis buffer (Beyotime Institute of Biotechnology, Shanghai, China), supplemented with protease inhibitors (1:100). The protein concentration was determined by BCA Protein Assay Kit (Dalian Meilun Biotechnology Co., Ltd, Dalian, China). 30 μg of proteins per sample was loaded in 10% sodium dodecyl sulfate-polyacrylamide gel electrophoresis (SDS-PAGE) and transferred onto polyvinylidene fluoride (PVDF) membranes (Millipore corporation, USA). After being blocked with TBST containing 5% skim milk for 1 h, and then was incubated overnight at 4 °C with specific primary antibodies including AKT (Cell Signaling Technology), PI3K (Cell Signaling Technology), FAK(Cell Signaling Technology), eNOS (abcam) and β-actin (Proteintech). Subsequently, the membrane was rinsed with TBST for three times and was exposed to suitable secondary HRP-conjugated antibodies at room temperature for 1.5 h. The ECL (Millipore corporation, USA) was used for signal detection. Blot data were analyzed with Image-Pro Plus 6.0 (Media Cybernetics, USA). Gray values of blot areas are measured, and the relative expression amount of the protein samples is calculated by the method of the target protein gray value/internal reference β-actin gray value.

Quantitative Real-time PCR

Total RNA was extracted from HUVECs with RNAprep Pure Micro Kit (Tiangen Biotech (Beijing) Co., Ltd, Beijing, China) according to the manufacturer's protocol. Total RNA were quantified with NanoDrop One (Thermo Fisher Scientific, USA) and reverse transcribed using 5X All-In-One RT MasterMix (Tiangen Biotech (Beijing) Co., Ltd, Beijing, China). qRT-PCR was performed on a QuantStudio 5 (Thermo Fisher Scientific, USA) using a TB Green™ Premix Ex Taq™ II kit (Takara, Japan) to measure and analyze the expression of specific genes. Reverse transcription and amplification conditions followed the reagent. Data were analyzed via the $2^{-\Delta\Delta Ct}$ method normalized to β-actain. Sequences of primers were used as follows from 5'to 3'extremity:

AKT: CTGCACAAACGAGGGGAGTA (F); GCGCCACAGAGAAGTTGTTG(R). PI3K: CCCAGGTGGAATGAATGGCT (F); GCCAATGGACAGTGTTCCTCT (R).

FAK: GCTCCCTTGCATCTTCCAGT (F); AATACTGGCCCAGGTGGTTG (R).

eNOS: GCCGGAACAGCACAAGAGTTAT (F); AGCCCGAACACACAGAACC (R)

β-actain : CTCACCATGGATGATGATATCGC (F); AGGAATCCTTCTGACCC-

ATGC (R).

Statistical Analysis

SPSS statistics 22.0 software (IBM, Armonk, NY, USA)) was used for statistical analysis. The data were expressed as the mean ± SEM. Multiple-group comparisons were analyzed using one-way analysis of variance followed by the Tukey post hoc multiple range test. $P < 0.05$ was considered to indicate a statistically significant difference.

Results

PPR administration significantly alleviated the development of atherosclerosis.

To examine whether PPR could inhibit the process of atherosclerotic lesions, we first assessed overall burden and distribution of atherosclerosis. As shown in Fig. 1a,c, oil red O positive area, particularly the area of the aortic arch, was significantly increased in model group compared with the control group. However, PPR treatment could notably decrease the size of plaque lesions of the whole aorta. As the burden of atheroma plaques in the aortic sinus was another important indicator used for evaluating the severity of atherosclerosis, we then analyzed paraffin sections of the aortic sinus. As shown in results (Fig. 1b, d, e, and f), model group mice aortic roots exhibited significant formation of atherosclerosis plaque, and a mass of foam cells and cholesterol crystals in the plaque. The aorta intima was serious lesions, and collagen and elastic fibers decreased in various degree. Encouragingly, the pathological changes of aortas were repressed by PPR, and the improvement effect in PPR-treated mice was similar to that in mice with rosuvastatin. In addition, we also measured the lipid level of mice. Compared to control group, ApoE$^{-/-}$ mice elevated TC,TG, LDL-C, and AI dramatically, but reduced HDL-C. PPR downgraded the levels of TC, TG, LDL-C, and AI, and restored the concentration of HDL-C similar to rosuvastatin (Fig. 2a). The results showed that the PPR had better controlling functions on dyslipidemia.

The Regulatory Effects of PPR on secretion fuction of vessel endothelium in serum.

Atherosclerosis is associated with impaired endothelial function that precedes structural vascular change. Therefore, we next investigated the effect of PPR on vascular function in ApoE$^{-/-}$ mice. ET-1 and NO plays crucial roles in maintaining basic vascular tension and cardiovascular system homeostasis. Under pathological conditions, the production of NO decreases after changing in the activity of eNOS,

leading to the occurrence and development of cardiovascular diseases. Compared to the control group, ET-1 was significantly up-regulated and eNOS significantly down-regulated in the model group (p<0.01). After drug intervention, the concentration of ET-1 was reduced by PPR and rosuvastatin (p<0.05) (Fig. 2B). PPR could increase eNOS content(p<0.05), but no change was confirmed by rosuvastatin. PGI_2 and TAX_2 are vasoactive substances released by vascular endothelial cells. The balance between PGI_2 and TAX_2 is an important influence on vascular wall tension. From the experimental results, it can be seen that the imbalance between PGI2 and TAX2 can be restored by PPR rather than rosuvastatin (Fig. 2b).

PPR improves the low shear stress-induced cell function damage.

VECs appear to sense shear stress of vascular cavity surface and transduce mechanical signal, which can regulate various signaling pathways and physiological functions [18]. Fluid shear stress is an important regulator of VECs functions [19]. In regions where the flowing blood is multidirectional (low shear stress or disturbed flow), VECs are activated and atherosclerotic plaque is detected [20]. Therefore, we used fluid shear system to induce VECs injury in vitro, in order to explored whether PPR can antagonize the low shear stress-induced cell function damage. We first carried out cell proliferation experiments (Fig. 3c). The results indicated that the low shear stress-induced cell increased cell excessive proliferation. However, the cells treated with PPR could inhibit cell excessive proliferation. Next, we tested the effects of PPR on endothelial cell migration (Fig. 3a,d). We observed decreased migration of HUVECs under low shear stress conditions (p<0.01), and cells migration increased after PPR treatment (p<0.05). Third, we examined the formation of capillary-like tubules on the Matrigel matrix to elucidate the angiogenesis potential (Fig. 3b, e, and f). The PPR group showed significant tube formation activity compared to the L-FSS group. These results suggested that PPR improved the cellular function damaged by low shear stress.

siRNA targeting Piezo1 offsets the protective effect of PPR on HUVECs

Piezo1, which is a sensor of shear stress, can sense the change of shear force on VECs. VECs responsiveness to shear stress is essential for vasoregulation and plays a role in atherogenesis [21]. Piezo1 is an important target for regulating VECs function and maintaining cardiovascular homeostasis. Loss of Piezo1 in endothelial cells leads to decrease of the cell's response to shear stress, disorder of alignment in the direction of flow and damage cell function [14, 22]. Therefore, to explore whether the protective effect of PPR connected with Piezo1, We silenced Piezo1 expression in HUVECs by siRNA. The result of qRT-PCR showed that the Piezo1 had been knocked out after the transfection with siRNA (Fig. 4a).First of all, we found that the morphology of Piezo1-silenced HUVECs changed from a cobblestone-like to spindle-shaped cells,and the cells arrangement changed from random to orderly. Cells morphology of Piezo1 siRNA + L-FSS group changed from a cobblestone-like to irregular shape and showed aggregation of F-actin filaments, suggesting that the cytoskeletal rearrangement and cells damage (Fig. 4c). Secondly, Knockdown of Piezo1 in HUVECs stimulated cell proliferation (Fig. 4b) and decreased cell migration (Fig. 4d, f) and tubular structure (Fig. 4e, g, h). We also could detect more cell damage in Piezo1 siRNA + L-FSS group. However, results showed that the protective effect of PPR was

remarkably abolished by these pretreatments. These results suggest that Piezo1 may be involved in the protective effect of PPR against HUVECs injury.

PPR Protected HUVECs By Activating FAK-PI3K/Akt Signaling Pathway

PI3K/Akt signaling pathway plays essential roles in the proliferation, migration and apoptosis of VECs [23, 24]. It also plays an important role in improving endothelial function and reducing atherosclerosis [25, 26]. Thus, we detected the expression levels of PI3K and Akt in HUVECs. As shown in Fig. 5a,b, compared with the static culture group, the expression of PI3K and Akt were significantly decreased by low shear stress pretreatment. However, decreased expression of PI3K and Akt was reversed in PPR-treated HUVECs. Previous study had reported that PI3K/Akt are key enzymes controlling eNOS phosphorylation, and blocking of PI3K/Akt can partially inhibit eNOS activity [27–29]. We also found that the activity of eNOS increased with the increase of PI3K / Akt expression in L-FSS + PPR group (Fig. 5c). PI3K has also been shown to bind FAK leading to activation of PI3K and its downstream effectors [30]. Therefore, we investigated the effects of PPR on low shear stress-induced expression of FAK. We found that FAK levels were significantly raised by the PPR-treated compared to the L-FSS group (Fig. 5d). These results suggested that PPR might activate FAK-PI3K/Akt pathway to protect HUVECs against low shear stress-induced injury.

To assess whether the activation effect of PPR on FAK-PI3K/Akt pathway is related to Piezo1, we used Piezo1 siRNA to knock down Piezo1. The result of qRT-PCR showed that the Piezo1 had been knocked out after the transfection with siRNA (Fig. 5). As shown in Fig. 5, results showed that the activation effect of PPR was abolished in varying degrees when Piezo1 was silenced by siRNA. We can infer that the Piezo1 involved in the protective effect of PPR against HUVECs injury.

Discussion

Atherosclerosis is a vascular chronic inflammatory disease resulting from lipid-deposited vascular wall with rupture-prone plaque and changes in structure and function of the vascular wall [31, 32]. Drugs that treat atherosclerosis usually act nonspecifically. The majority was taking a statin, antiplatelet therapy, beta-blocker, or angiotensin converting enzyme inhibitor/angiotensin receptor blocker [33]. However, these drugs have some side effects such as rhabdomyolysis and conduction block. Moreover, atherosclerosis is a sophisticated disease of uncertain cause. Single target cure is not enough for an effective antibacterial therapy. TCM, with the characteristics of syndrome differentiation, has unique advantages in the treatment or prevention of atherosclerosis. Many classic prescriptions or active ingredients of single herb can effectively prevent atherosclerosis, reduce the incidence of cardiovascular events, and treat atherosclerosis with a wide range of applications. Fufang Danshen formula is the clinically important anti-atherosclerosis drugs. It has the characteristics of multi-component, multi-target, and multi-channel. Many scholars have conducted a series of studies based on different target molecules in order to dissect out the exact mechanism of action of Fufang Danshen formula [34]. Due to complex composition of

Fufang Danshen formula, preliminary work of our group has screened out the best combination of active ingredients in order to clarify the mechanism of anti atherosclerosis, namely Rg1, R1, and PCAD.

The current study demonstrates the anti-atherosclerotic effects of PPR in ApoE$^{-/-}$mice. As we expected, PPR was able to significantly reduce atherosclerotic area and lipid level compared with model group mice. Endothelial dysfunction plays an important role in atherosclerosis development. Our data showed that the expression of was ET-1 and TAX2 decreased and that of eNOS and PGI2 was increased. These results suggested that the endothelial damage is repaired in ApoE-/- mice. The in vivo assay prompted us to explore its underlying mechanism of endothelial protection.

VECs dysfunctions have been found to play vital roles in the initiation of vascular disorders and atherosclerosis [35] and results in the earliest detectable changes in the life history of an atherosclerotic lesion [36, 37]. Low shear stress is an important risk factor for VECs injury [38, 39]. In the present study, we demonstrated that PPR could ameliorate low shear stress-induced HUVECs dysfunctions. PPR significantly repaired cell morphology, reduced cell excessive proliferation and ameliorated migration and tube formation activity.

PI3K/Akt signaling pathway, as a variety of vascular growth factors, regulates diverse cellular activities related to cell growth, metabolism, migration, and apoptosis [40, 41]. Previous studies have reported that PI3K/Akt is known to be a major regulator of proliferation, migration and survival of VECs as well as vascular permeability [42]. Moreover, it have been previously confirmed that PI3K/Akt pathway can mediate the shear-induced signaling [43]. Interfering the PI3K/Akt signaling pathway has been an effective strategy to inhibit endothelial dysfunction. In the present study, we confirmed that PPR treatment increases the expression of PI3K and Akt. Akt is an important regulator of eNOS activity in vessels [44]. eNOS regulates the release of NO to promote VECs migration and neovascularization [45]. In our data, the use of PPR can regulated the expression of Akt and thus increased eNOS in low shear stress-treated HUVECs. FAK is a cytoplasmic non-receptor protein tyrosine kinase that plays a key role in regulating cell migration [46]. The activation of FAK, as a primary signalling mediator, is required for focal adhesion turnover and actin cytoskeletal dynamic reorganisation in cell migration [47]. In addition, FAK has been shown to activate the PI3K/Akt signaling pathway [48, 49]. Therefore, we detected the expression of FAK. Our results showed that PPR increased the level of FAK, meaning that PPR promoted the FAK and thus enhanced expression of PI3K and Akt. Therefore, we deduced that PPR could play a role in protecting VECs by intervene FAK- PI3K/Akt signaling pathway.

Piezo1 protein has been identified as an essential component of mechanically activated channels and induces cationic non-selective mechanically activated currents [14, 50]. Piezo1 channels have been revealed to be sensors of blood flow through shear-stress-evoked ionic current and calcium influx in endothelial cells [22]. Shear stress is the main physiological stimulus that causes the endothelium to release vasoactive factors and regulate vascular tone [51]. Research has suggested that laminar shear stress can activate Piezo1and modulate NO release from endothelium activity so as to maintain vascular tension of local blood vessels [15]. To explore whether the protective effect of PPR connected with

Piezo1, we pretreated HUVECs with silenced Piezo1 expression by siRNA. Results showed that Piezo1 siRNA could abolish the protective effects of PPR. These results suggest that Piezo1 are indeed involved in the protective effect of PPR against low shear stress-induced cells dysfunctions.

Our study also has several limitations. There is a growing interest in therapy using Chinese medicine that affects several targets/pathways. This study only focused on the effects of PPR on FAK- PI3K/Akt signaling pathway and its influence on VECs function. However, its role in other signaling pathways related to the pathogenesis of atherosclerosis and other vascular cell types has not been fully explored. Although, it is significant change in the efficacy of the PPR by Piezo1 siRNA, the specific mechanism is still not clear.

Conclusion

In summary, our study provided evidence that PPR exerts excellent effects on the complicated atherogenic condition. PPR has a positive role in improves cellular function by low shear stress injury which is related to the intervene FAK- PI3K/Akt signaling pathway, reduced cell excessive proliferation, ameliorated migration and tube formation activity, effectively inhibiting vascular injury. Piezo1 is a possible target of PPR in the treatment of atherosclerosis. Our results provide a new insight for the treatment of atherosclerosis.

Abbreviations

MACEs: major adverse cardiovascular events; VECs: vascular endothelium cells; PI3K: Phosphatidylinositol 3-kinase; eNOS: nitric oxide synthase; NO: produce nitric oxide; Rg1: Ginsenoside Rg1, R1: Notoginsenoside R1; PCAD: Protocatechuic aldehyde; PPR: Rg1-Notoginsenoside R1-Protocatechuic aldehyde; TC: total cholesterol; TG triglyceride; HDL-C: high-density lipoprotein cholesterol; LDL-C: low-density lipoprotein cholesterol; AI: atherosclerosis index; ET-1: endothelin-1; PGI_2: Prostaglandine2: TXA_2: ThromboxaneA2; ELISA: enzyme-linked immunosorbent assay; ECM: endothelial cell medium; RT: room temperature; SDS-PAGE: sodium dodecyl sulfate-polyacrylamide gel electrophoresis; PVDF: transferred onto polyvinylidene fluoride.

Declarations

Ethics approval and consent to participate

All animal studies were approved by the Animal Ethics Committee of Shandong University of Traditional Chinese Medicine.

Consent for publication

Not applicable.

Availability of data and materials

The all original data supported the findings of this study were supplied by Wenqing Yang under license and cannot be made freely available. Requests for access to these data should be made to Wenqing Yang, winnie0416q@163.com.

Competing interests

The authors declare that there are no conflicts of interest.

Funding

This study was supported by grants from the NSFC Youth Science Foundation Project (81804006), National Natural Science Foundation of China (81974566). This study was also supported by the Program of Scientific research projects in Universities of Shandong Province (J18KA260).

Authors' contributions

Lei Zhang and Yan Li participated in all experimental work and drafted the paper. Xin Ma and Xiaojie Wang were involved in the in vivo experiments. Lingxiao Zhang was involved in the in vitro experiments. Lei Zhang, Yan Li and Wenqing Yang were performed data analysis. Wenqing Yang and Yunlun Li were designed the experimental protocols.

Acknowledgements

Not applicable

References

1. Sanchis-Gomar F, Perez-Quilis C, Leischik R, Lucia A. Epidemiology of coronary heart disease and acute coronary syndrome. Ann Transl Med. 2016;4:256.
2. Li D, Liu Y, Zhang X, Lv H, Pang W, Sun X, Gan LM, Hammock BD, Ai D, Zhu Y. Inhibition of soluble epoxide hydrolase alleviated atherosclerosis by reducing monocyte infiltration in Ldlr(-/-) mice. J Mol Cell Cardiol. 2016;98:128–37.
3. Furuuchi R, Shimizu I, Yoshida Y, Hayashi Y, Ikegami R, Suda M, Katsuumi G, Wakasugi T, Nakao M, Minamino T. Boysenberry polyphenol inhibits endothelial dysfunction and improves vascular health. PLoS One. 2018;13:e0202051.
4. Drozdz D, Latka M, Drozdz T, Sztefko K, Kwinta P. Thrombomodulin as a New Marker of Endothelial Dysfunction in Chronic Kidney Disease in Children. Oxid Med Cell Longev. 2018;2018:1619293.
5. Szewczyk A, Jarmuszkiewicz W, Koziel A, Sobieraj I, Nobik W, Lukasiak A, Skup A, Bednarczyk P, Drabarek B, Dymkowska D, et al. Mitochondrial mechanisms of endothelial dysfunction. Pharmacol Rep. 2015;67:704–10.

6. Gimbrone MA Jr, Garcia-Cardena G. Vascular endothelium, hemodynamics, and the pathobiology of atherosclerosis. Cardiovasc Pathol. 2013;22:9–15.
7. Shimomura R, Nezu T, Hosomi N, Aoki S, Sugimoto T, Kinoshita N, Araki M, Takahashi T, Maruyama H, Matsumoto M. Alpha-2-macroglobulin as a Promising Biological Marker of Endothelial Function. J Atheroscler Thromb. 2018;25:350–8.
8. Gimbrone MA Jr, Garcia-Cardena G. Endothelial Cell Dysfunction and the Pathobiology of Atherosclerosis. Circ Res. 2016;118:620–36.
9. Rosenberg JH, Werner JH, Moulton MJ, Agrawal DK. Current Modalities and Mechanisms Underlying Cardioprotection by Ischemic Conditioning. J Cardiovasc Transl Res. 2018;11:292–307.
10. Chen J, Yuan H, Talaska AE, Hill K, Sha SH. Increased Sensitivity to Noise-Induced Hearing Loss by Blockade of Endogenous PI3K/Akt Signaling. J Assoc Res Otolaryngol. 2015;16:347–56.
11. Sadeghi N, Gerber DE. Targeting the PI3K pathway for cancer therapy. Future Med Chem. 2012;4:1153–69.
12. Hiob MA, Trane AE, Wise SG, Bernatchez PN, Weiss AS. Tropoelastin enhances nitric oxide production by endothelial cells. Nanomedicine (Lond). 2016;11:1591–7.
13. Faucherre A, Kissa K, Nargeot J, Mangoni ME, Jopling C. Piezo1 plays a role in erythrocyte volume homeostasis. Haematologica. 2014;99:70–5.
14. Ranade SS, Qiu Z, Woo SH, Hur SS, Murthy SE, Cahalan SM, Xu J, Mathur J, Bandell M, Coste B, et al. Piezo1, a mechanically activated ion channel, is required for vascular development in mice. Proc Natl Acad Sci U S A. 2014;111:10347–52.
15. Wang S, Chennupati R, Kaur H, Iring A, Wettschureck N, Offermanns S. Endothelial cation channel PIEZO1 controls blood pressure by mediating flow-induced ATP release. J Clin Invest. 2016;126:4527–36.
16. Hahn C, Schwartz MA. Mechanotransduction in vascular physiology and atherogenesis. Nat Rev Mol Cell Biol. 2009;10:53–62.
17. Albarran-Juarez J, Iring A, Wang S, Joseph S, Grimm M, Strilic B, Wettschureck N, Althoff TF, Offermanns S. Piezo1 and Gq/G11 promote endothelial inflammation depending on flow pattern and integrin activation. J Exp Med. 2018;215:2655–72.
18. Baeyens N, Bandyopadhyay C, Coon BG, Yun S, Schwartz MA. Endothelial fluid shear stress sensing in vascular health and disease. J Clin Invest. 2016;126:821–8.
19. McCormick SM, Seil JT, Smith DS, Tan F, Loth F. Transitional Flow in a Cylindrical Flow Chamber for Studies at the Cellular Level. Cardiovasc Eng Technol. 2012;3:439–49.
20. Le NT, Abe JI. **Regulation of Kir2.1 Function Under Shear Stress and Cholesterol Loading**. *J Am Heart Assoc* 2018, 7.
21. Choi HW, Barakat AI. Numerical study of the impact of non-Newtonian blood behavior on flow over a two-dimensional backward facing step. Biorheology. 2005;42:493–509.

22. Li J, Hou B, Tumova S, Muraki K, Bruns A, Ludlow MJ, Sedo A, Hyman AJ, McKeown L, Young RS, et al. Piezo1 integration of vascular architecture with physiological force. Nature. 2014;515:279–82.
23. Jiri, Polivka, Jr. Filip, Janku: **Molecular targets for cancer therapy in the PI3K/AKT/mTOR pathway**.
24. Shi H, Feng JM. Aristolochic acid induces apoptosis of human umbilical vein endothelial cells in vitro by suppressing PI3K/Akt signaling pathway. Acta Pharmacol Sin. 2011;32:1025–30.
25. García-Prieto CF, Hernández-Nu?o F, Rio DD, Ruiz-Hurtado G, Aránguez I, Ruiz-Gayo M, Somoza B, Fernández-Alfonso MS. **High-fat diet induces endothelial dysfunction through a down-regulation of the endothelial AMPK-PI3K-Akt-eNOS pathway**. *Molecular Nutrition & Food Research*, 59:520–532.
26. Wang R, Peng L, Zhao J, Zhang L, Guo C, Zheng W, Chen H. **Gardenamide A Protects RGC-5 Cells from H2O2-Induced Oxidative Stress Insults by Activating PI3K/Akt/eNOS Signaling Pathway**. *International Journal of Molecular Sciences*, 16:22350–22367.
27. Fleming I, Busse R. **Molecular mechanisms involved in the regulation of the endothelial nitric oxide synthase: Fig. 1**. *Am J Physiol Regul Integr Comp Physiol*, 284:R1-R12.
28. Fulton D, Gratton JP, Sessa WC. Post-translational control of endothelial nitric oxide synthase: Why isn't calcium/calmodulin enough? Journal of Pharmacology Experimental Therapeutics. 2002;299:818–24.
29. Zhang YM, Qu XY, Zhai JH, Tao LN, Gao H, Song YQ, Zhang SX. **Xingnaojing Injection Protects against Cerebral Ischemia Reperfusion Injury via PI3K/Akt-Mediated eNOS Phosphorylation**. *Evidence Based Complementary & Alternative Medicine*, 2018:1–13.
30. Seguin L, Desgrosellier JS, Weis SM, Cheresh DA. **Integrins and cancer: regulators of cancer stemness, metastasis, and drug resistance**. *Trends in Cell Biology*, 25:234–240.
31. Taleb S, Tedgui A, Mallat Z. **IL-17 and Th17 Cells in Atherosclerosis Subtle and Contextual Roles**. *Arteriosclerosis Thrombosis & Vascular Biology* 2014, 35.
32. Zamaklar M, Lalić K, Lalić N. [Vascular inflammation: effect of proatherogenic dyslipidemic trio or quartet]. Med Pregl. 2009;62(Suppl 3):37–42.
33. Vedin O, Hagstrom E, Stewart R, Brown R, Krug-Gourley S, Davies R, Wallentin L, White H, Held C. **Secondary prevention and risk factor target achievement in a global, high-risk population with established coronary heart disease: baseline results from the STABILITY study**. *European Journal of Preventive Cardiology*, 20:678–685.
34. Zhou Z, Liu Y, Miao A-D, Wang S-Q. **Protocatechuic aldehyde suppresses TNF-α-induced ICAM-1 and VCAM-1 expression in human umbilical vein endothelial cells**. 513:1–8.
35. Mundi S, Massaro M, Scoditti E, Carluccio MA, Caterina RD. Endothelial Permeability, Ldl Deposition, and Cardiovascular Risk Factors - A Review. Cardiovasc Res. 2017;114:35.
36. Stary HC. Natural History and Histological Classification of Atherosclerotic Lesions: An Update. Arterioscler Thromb Vasc Biol. 2000;20:1177–8.
37. Virmani R, Kolodgie FD, Burke AP, Farb A, Schwartz SM. Lessons from sudden coronary death: a comprehensive morphological classification scheme for atherosclerotic lesions. Arterioscler Thromb

Vasc Biol. 2000;20:1262–75.

38. Man HSJ, Sukumar AN, Lam GC, Turgeon PJ, Yan MS, Ku KH, Dubinsky MK, Ho JJD, Wang JJ, Das S, et al. Angiogenic patterning by STEEL, an endothelial-enriched long noncoding RNA. Proc Natl Acad Sci U S A. 2018;115:2401–6.
39. Baeriswyl DC, Prionisti I, Peach T, Tsolkas G, Chooi KY, Vardakis J, Morel S, Diagbouga MR, Bijlenga P, Cuhlmann S, et al. Disturbed flow induces a sustained, stochastic NF-kappaB activation which may support intracranial aneurysm growth in vivo. Sci Rep. 2019;9:4738.
40. Whiteman EL, Han C, Birnbaum MJ. **Role of Akt/protein kinase B in metabolism**. *Trends Endocrinol Metab*, 13:0–451.
41. Cantley LC. **The Phosphoinositide 3-Kinase Pathway**. *Science*, 296:1655–1657.
42. Cui H-J, Yang A-L, Zhou H-J, Wang C, Luo J-K, Lin Y, Zong Y-X, Tang T. **Buyang huanwu decoction promotes angiogenesis via vascular endothelial growth factor receptor-2 activation through the PI3K/Akt pathway in a mouse model of intracerebral hemorrhage**. *Bmc Complementary & Alternative Medicine*, 15:91.
43. Li YSJ, Haga JH, Chien S. **Molecular basis of the effects of shear stress on vascular endothelial cells**. 38:1949–1971.
44. Ahsan A, Han G, Pan J, Liu S, Padhiar AA, Chu P, Sun Z, Zhang Z, Sun B, Wu J, et al. Phosphocreatine protects endothelial cells from oxidized low-density lipoprotein-induced apoptosis by modulating the PI3K/Akt/eNOS pathway. Apoptosis. 2015;20:1563–76.
45. Fu R, Wang Q, Guo Q, Xu J, Wu X. **XJP-1 protects endothelial cells from oxidized low-density lipoprotein-induced apoptosis by inhibiting NADPH oxidase subunit expression and modulating the PI3K/Akt/eNOS pathway**. *Vascul Pharmacol*, 58:78–86.
46. Zhao X, Guan JL. Focal adhesion kinase and its signaling pathways in cell migration and angiogenesis. Adv Drug Deliv Rev. 2011;63:610–5.
47. Cheng L, Xu J, Qian YY, Pan HY, Yang H, Shao MY, Cheng R, Hu T. **Interaction between mDia1 and ROCK in Rho-induced migration and adhesion of human dental pulp cells**. *International Endodontic Journal*:n/a-n/a.
48. Horowitz JC, Rogers DS, Sharma V, Vittal R, White ES, Cui Z, Thannickal VJ. **Combinatorial activation of FAK and AKT by transforming growth factor-β1 confers an anoikis-resistant phenotype to myofibroblasts**. 19:761–771.
49. Garth G. Steven, Huang, Katsuhide, Okunishi, Jacob, Scott: **Reversal of myofibroblast differentiation by prostaglandin E(2)**. *American Journal of Respiratory Cell & Molecular Biology*.
50. Volkers L, Mechioukhi Y, Coste B. Piezo channels: from structure to function. Pflugers Arch. 2015;467:95–9.
51. Dehghan B, Sabri MR, Javanmard SH, Ahmadi AR, Mansourian M. Neurally mediated syncope: Is it really an endothelial dysfunction? Anatol J Cardiol. 2016;16:701–6.

Figures

Figure 1

The effects of PPR on the development of atherosclerosis. a Representative Oil-red O staining of the entire aorta. b Representative images of H&E, Masson and Movat staining from the aortic root (Magnification, ×50). c Quantification of the en face lesion area of the entire aorta. d Percentage of aortic plaque area. (aortic plaque area%). (e) Percentage of collagen content collagen fiber content). f Percentage of elastin plaque area (elastin per plaque). The data was expressed as the mean ± SD, n = 6 for each group. ∗p < 0.05 vs. the model group.

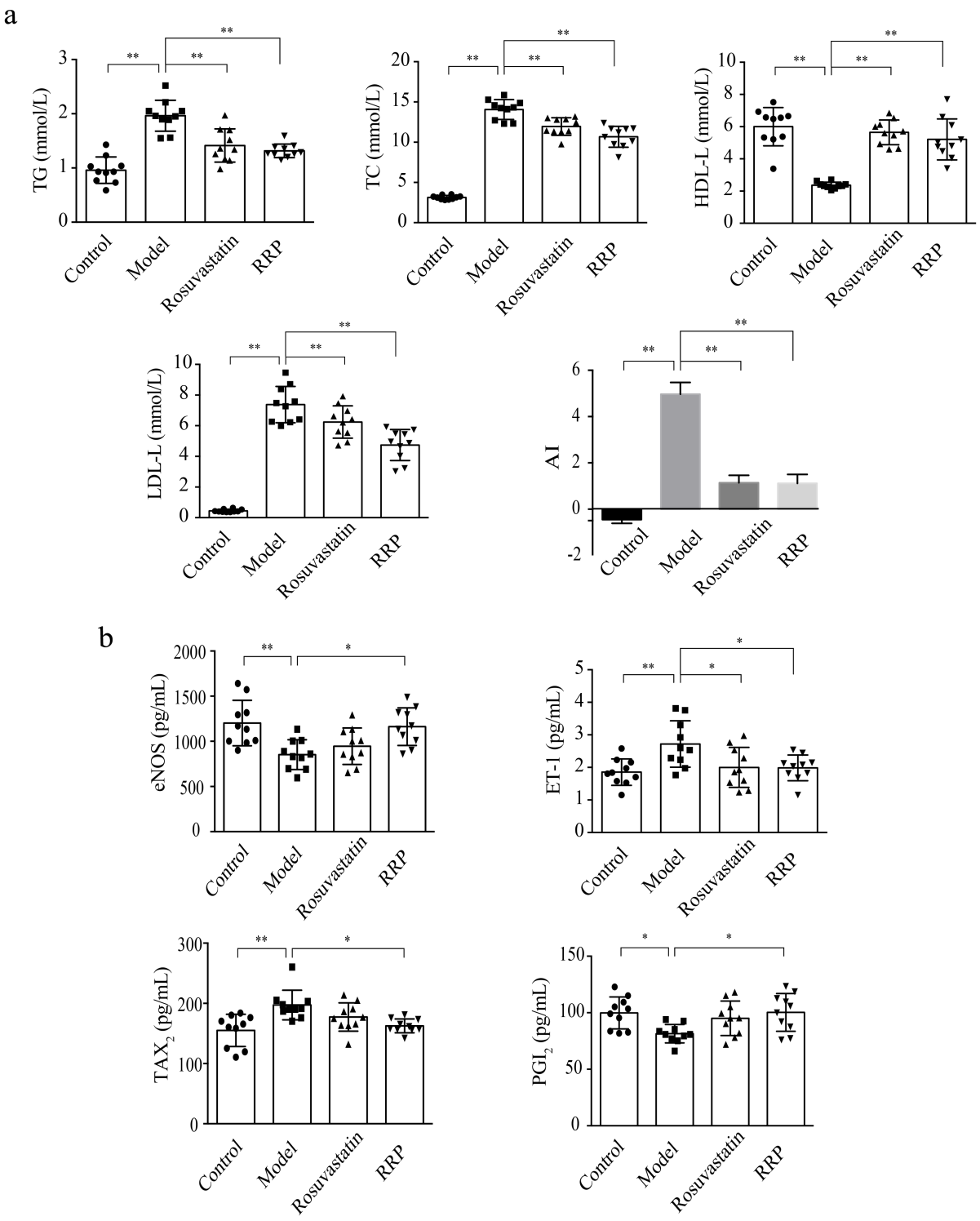

Figure 2

The effects of PPR on lipids and secretion faction of vessel endothelium in serum. a Levels of serum lipids (TG, TC, LDL-C, and HDL-C) in mice. b Levels of eNOS, ET-1, PGI2, and TXA2 in mice. The data was expressed as the mean ± SD, n = 10 for each group. ∗p < 0.05, ∗∗p < 0.001 vs. the model group.

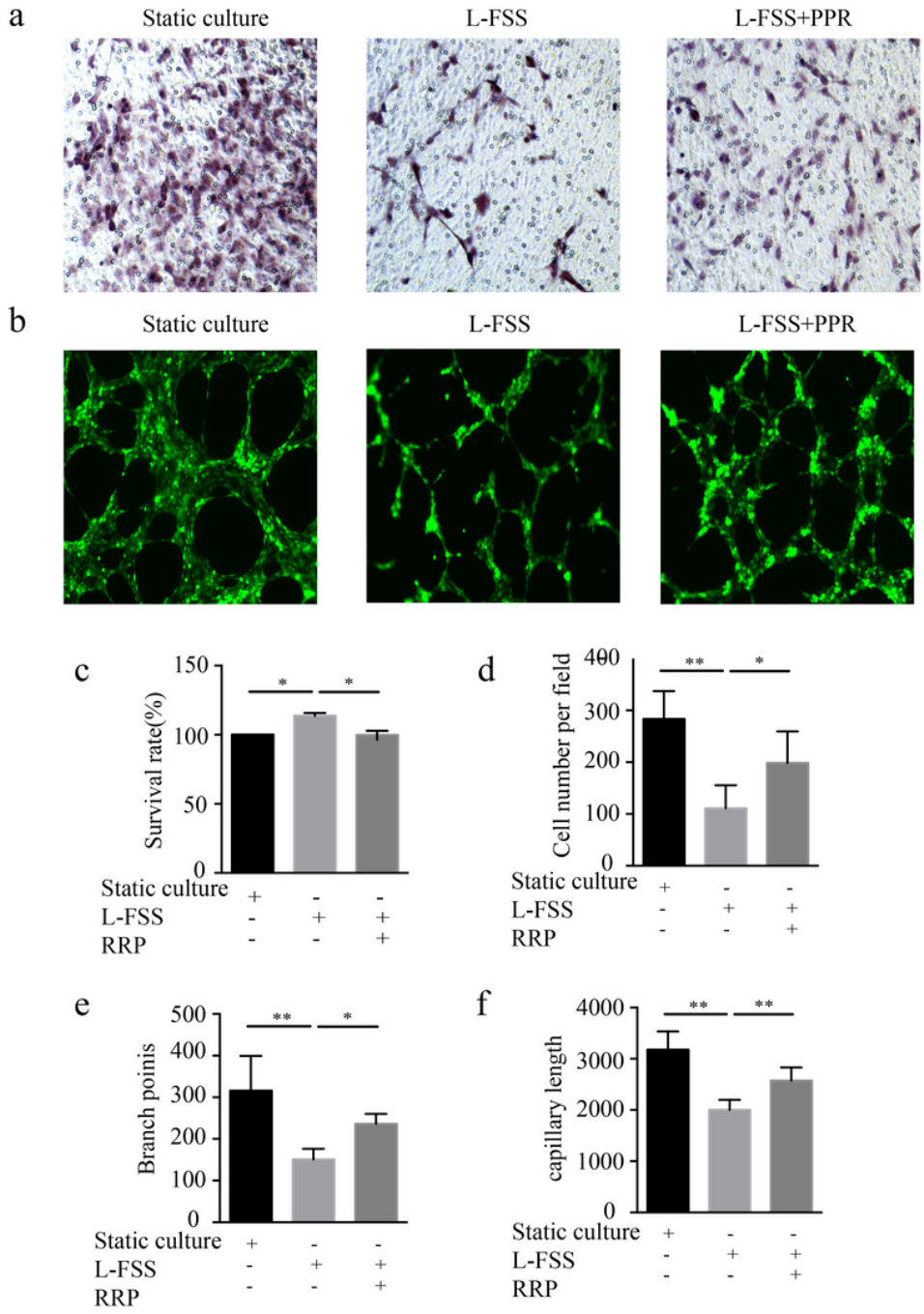

Figure 3

PPR affected HUVECs proliferation, migration and tubule formation mediated. a, d Representative images of the migration of HUVECs and the calculated cellVmigration number, scale bars = 50 μm, *p < 0.05, **p < 0.001 vs. L-FSS group. b Representative images of the formation of capillary-like tubules in HUVECs, scale bars = 200 μm. c Proliferation activity of HUVECs, *p < 0.05 vs. L-FSS group. e, f Capillary morphogenesis was quantified by calculating the branch poinis (e) and capillary length (f), *p < 0.05, **p < 0.001 vs. L-FSS group.

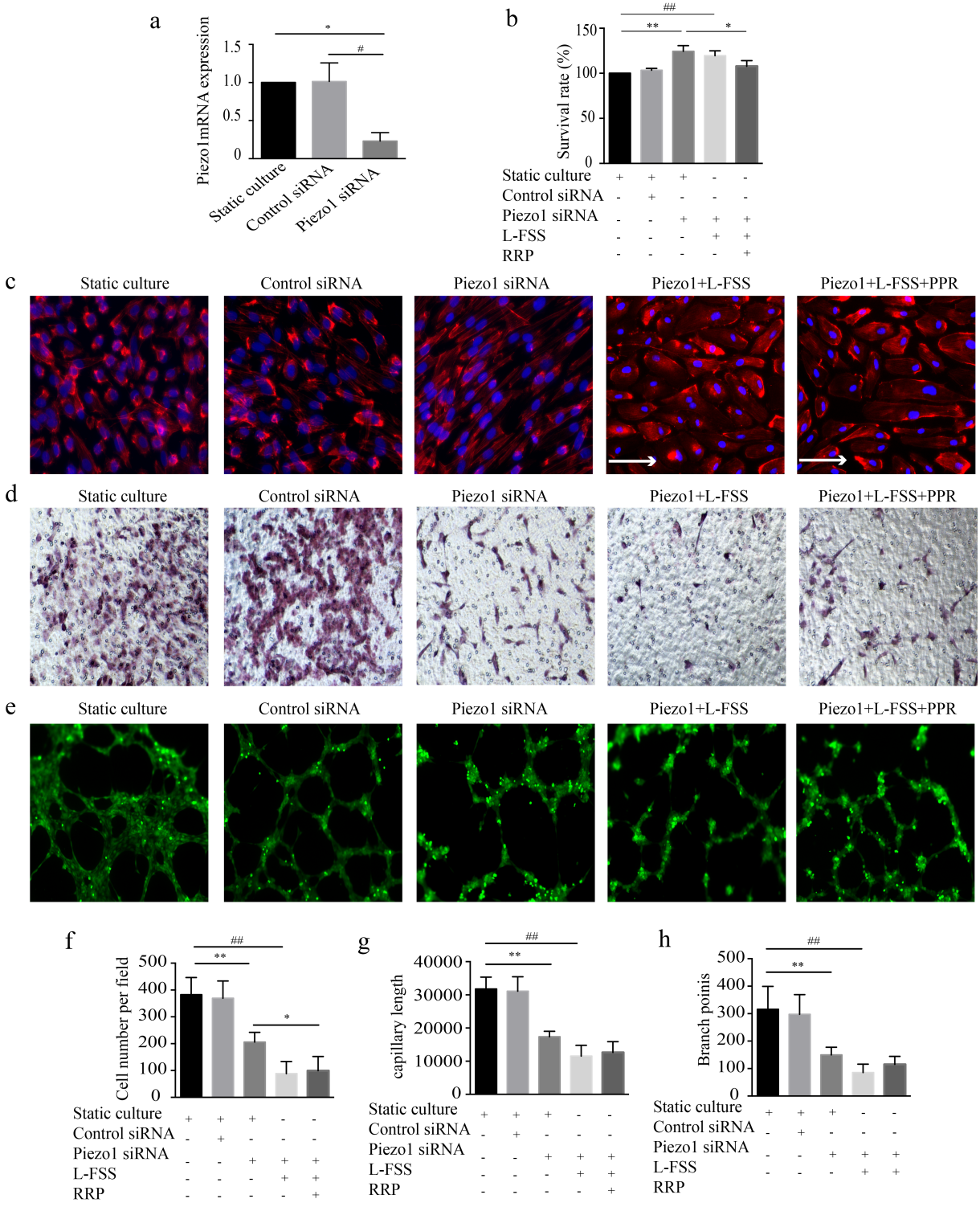

Figure 4

Inhibition of Piezo1 using siRNA abrogated the protective effects of PPR on HUVECs injury. a The mRNA expression of Piezo1 detected by qRT-PCR in indicated groups. b Proliferation activity of HUVECs, *p < 0.05 vs. Piezo1 siRNA group. c Cellular alignment was analyzed by staining cells with phalloidin (red) and DAPI (blue)，scale bars = 50 μm, arrows indicate the fluid direction. d, f Representative images of the migration of HUVECs and the calculated cell migration number, scale bars = 50 μm, *p < 0.05, **p < 0.001

vs. Piezo1 siRNA group, ##p < 0.001 vs. Piezo1 siRNA+L-FSS group. (e) Representative images of the formation of capillary-like tubules in HUVECs, scale bars = 200 μm. g, h Capillary morphogenesis was quantified by calculating the branch poinis (g) and capillary length (h), **p < 0.001 vs. Piezo1 siRNA group, #p < 0.05, ##p < 0.001 vs. Piezo1 siRNA+L-FSS group.

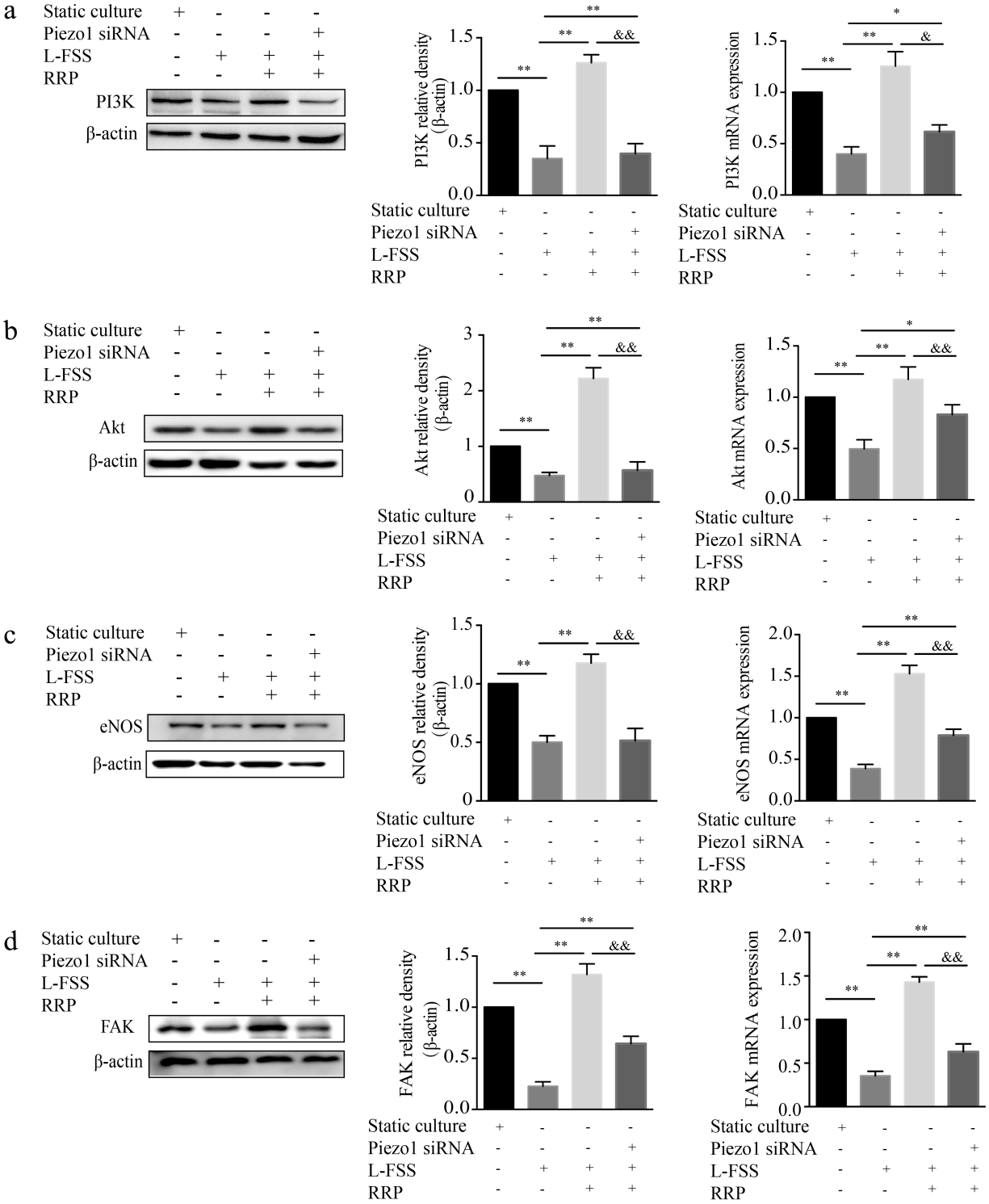

Figure 5

Effects of PPR on FAK-PI3K/Akt pathway. a The mRNA levels of PI3K by qPCR and Western Blot results of PI3K. b The mRNA levels of Akt by qPCR and Western Blot results of Akt. c The mRNA levels of eNOS by qPCR and Western Blot results of eNOS. d The mRNA levels of FAK by qPCR and Western Blot results of FAK. *p < 0.05, **p < 0.001 vs. L-FSS group□&p < 0.05, &&p < 0.001 vs. L-FSS+PPR group